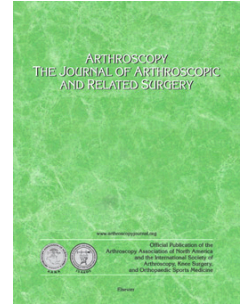


Journal Pre-proof

Assessing the Resident Progenitor Cell Population and the Vascularity of the Adult Human Meniscus

Jorge Chahla, MD PhD, Angela Papalamprou, PhD, Virginia Chan, BS, Yasaman Arabi, BS, Khosrawdad Salehi, BS, Trevor J. Nelson, BS, Orr Limpisvasti, MD, Bert R. Mandelbaum, MD DHL, Wafa Tawackoli, PhD, Melodie F. Metzger, PhD, Dmitriy Sheyn, PhD



PII: S0749-8063(20)30754-4

DOI: <https://doi.org/10.1016/j.arthro.2020.09.021>

Reference: YJARS 57135

To appear in: *Arthroscopy: The Journal of Arthroscopic and Related Surgery*

Received Date: 10 March 2020

Revised Date: 9 September 2020

Accepted Date: 10 September 2020

Please cite this article as: Chahla J, Papalamprou A, Chan V, Arabi Y, Salehi K, Nelson TJ, Limpisvasti O, Mandelbaum BR, Tawackoli W, Metzger MF, Sheyn D, Assessing the Resident Progenitor Cell Population and the Vascularity of the Adult Human Meniscus, *Arthroscopy: The Journal of Arthroscopic and Related Surgery* (2020), doi: <https://doi.org/10.1016/j.arthro.2020.09.021>.

This is a PDF file of an article that has undergone enhancements after acceptance, such as the addition of a cover page and metadata, and formatting for readability, but it is not yet the definitive version of record. This version will undergo additional copyediting, typesetting and review before it is published in its final form, but we are providing this version to give early visibility of the article. Please note that, during the production process, errors may be discovered which could affect the content, and all legal disclaimers that apply to the journal pertain.

© 2020 Published by Elsevier on behalf of the Arthroscopy Association of North America

Assessing the Resident Progenitor Cell Population and the Vascularity of the Adult Human Meniscus

Jorge Chahla, MD PhD^{1*}, Angela Papalamprou, PhD^{2,3*}, Virginia Chan, BS^{2,3}, Yasaman Arabi, BS^{2,3}, Khosrawdad Salehi, BS^{2,3}, Trevor J. Nelson, BS⁴, Orr Limpisvasti, MD¹, Bert R Mandelbaum, MD DHL¹, Wafa Tawackoli, PhD,^{2,3,5,6} Melodie F. Metzger, PhD⁴, Dmitriy Sheyn, PhD^{1,2,4,5,6#}

¹Kerlan Jobe Institute, ²Orthopedic Stem Cell Research Laboratory, ³Board of Governors Regenerative Medicine Institute, ⁴Department of Orthopedics, ⁵Department of Surgery, ⁶Department of Biomedical Sciences, Cedars-Sinai Medical Center, Los Angeles, CA.

*JC and AP contributed equally to this study.

To whom the correspondence should be addressed

Dmitriy Sheyn, PhD
Assistant Professor
Orthopedic Stem Cell Research Lab
Board of Governors Regenerative Medicine Institute
Department of Orthopedics
Department of Surgery
Department of Biomedical Sciences
Cedars-Sinai Medical Center
8700 Beverly Blvd. AHSP A8308
Los Angeles, CA, 90048
Office: 424-3154579

ACKNOWLEDGMENTS

This study was funded by The American Orthopaedic Society for Sports Medicine 2018 Young Investigator Grant # YIG-2018-1 to (JC). The authors acknowledge the Joint Restoration Foundation (JRF, Centennial, CO), Musculoskeletal Transplant Foundation (MTF, Edison, NJ) and Biosource Medical (Lakeland, FL) for generously providing the allografts used in this study, the biobank and translational research core for the histological analysis. The authors wish to acknowledge Cedars-Sinai Biobank and Translational Research Core for performing the histological analysis and scanning the slides. The authors acknowledge NIH/NIAMS K01AR071512 funding to DS. Authors also wish to thank Julia Sheyn for the help with image processing.

1 **Abstract**

2 **Purpose:** To identify, characterize, and compare the resident progenitor cell populations within
3 the red-red (RR), red-white (RW) and white-white (WW) zones of freshly harvested human
4 cadaver menisci and to characterize the vascularity of human menisci using
5 immunofluorescence and three dimensional (3D) imaging.

6 **Methods:** Fresh adult human menisci were harvested from healthy donors. Menisci were
7 enzymatically digested, mononuclear cells isolated and characterized using flow cytometry with
8 antibodies against MSCs surface markers (CD105, CD90, CD44 and CD29). Cells were
9 expanded in culture, characterized and compared to bone marrow-derived mesenchymal stem
10 cells (BM-MSCs). Trilineage differentiation potential of cultured cells was determined.
11 Vasculature of menisci was mapped in 3D using a modified uDisco clearing and
12 immunofluorescence against vascular markers CD31, lectin and alpha smooth muscle actin
13 (α SMA).

14 **Results:** There were no significant differences in the clonogenicity of isolated cells between the
15 three zones. Flow cytometry showed presence of CD44⁺CD105⁺CD29⁺CD90⁺ cells in all three
16 zones with high prevalence in the WW zone. Progenitors from all zones were found to be potent
17 to differentiate to mesenchymal lineages. Larger vessels in the RR zone of meniscus were
18 observed spanning towards RW, sprouting to smaller arterioles and venules. CD31⁺ cells were
19 identified in all zones using the 3D imaging and co-localization of additional markers of
20 vasculature (lectin and α SMA) was observed.

21 **Conclusion:** The presence of resident mesenchymal progenitors was evident in all three
22 meniscal zones of healthy adult donors without injury. Additionally, our results demonstrate the
23 presence of vascularization in the WW zone.

24 **Clinical Relevance:** The existence of progenitors and presence of microvasculature in the WW
25 zone of the meniscus suggests the potential for repair and biologic augmentation strategies in
26 that zone of the meniscus in young healthy adults. Further research is necessary to fully define
27 the functionality of the meniscal blood supply and its implications for repair.

28 **INTRODUCTION**

29 Prognosis following meniscal injuries is highly variable depending upon the size and location of
30 the tear. Some reports state that if the lesion communicates with the peripheral one-third of the
31 meniscus, increased vascularity may help it heal and therefore are more amenable for repairs.¹
32 Conversely, injuries in the “avascular” zone are almost always resected due to their low
33 potential success rate. Until recently it was believed that resecting a small percentage of
34 meniscus would not significantly impact joint longevity. However, a direct relationship between
35 the amount of meniscus resected and the presence/severity of chondral lesions in the ipsilateral
36 knee compartment in prospective NFL players with a previous medial and/or lateral
37 meniscectomy has previously been reported.² Meniscectomies have been reported to
38 significantly reduce the career lengths of professional athletes,³ while repairs carry high success
39 rates at long-term follow-up.⁴ Yet, since there are no randomized controlled trials to compare
40 meniscal repair to resection, it is not entirely clear whether repair or resection would be
41 favorable on a case-by-case basis.⁵ The resident stromal progenitor cell population and the
42 vascularization of the inner meniscus are not defined precisely in the literature and therefore
43 strategies for repair might be better informed if a more consistent approach was used to
44 characterize them.

45

46 Unlike highly vascularized bone tissue, fibrocartilaginous tissue has relatively limited self-repair
47 capacity. Previous studies suggest healing of inner meniscal tears can be enhanced through
48 progenitor cell mobilization⁶ and recruitment from the synovium, followed by formation of an
49 intermediate fibrous integration and cartilaginous remodeling.⁷ Kobayashi *et al*⁸ utilized an *in*
50 *vitro* organ culture model of freshly prepared defects to investigate the healing potential of the
51 rabbit meniscus without the influence of vascular supply. The authors found that grafts
52 integrated better in the peripheral outer region of the meniscus, suggesting that the endogenous
53 cellular composition of the meniscus may play a role in the local healing response. Progenitor
54 cells have been identified in the menisci of goats, rabbits and more recently in humans,⁹ which
55 suggests an inherent healing capacity. Mauck *et al* reported that resident meniscal
56 fibrochondrocytes from all regions of the meniscus possess a multilineage differentiation
57 capability, particularly toward chondrogenesis and adipogenesis in calf menisci.¹⁰ Since it is well
58 established that mechanical cues affect the development and maturation of the cellular milieu,¹¹
59 it is important to better understand the cellular content of human menisci. The progenitor

60 content between the different meniscal zones has not been investigated in adult human menisci,
61 most likely because of the scarcity of fresh human grafts made available for research purposes.
62 The intrinsic healing capacity of the meniscus is considered limited due to a poor blood supply
63 that only reaches the periphery of the meniscus.¹² King¹³ was the first to suggest that tears
64 extending to the vascular periphery undergo spontaneous repair, whereas tears limited to the
65 inner region do not. Seminal anatomical studies performed on human cadaveric menisci in the
66 1980s using injection techniques have established the current paradigm of meniscus
67 vascularity.¹ However, there is controversy in the literature regarding the specific topology of
68 meniscus vasculature as well as the specific timeline when the vasculature undergoes
69 developmental changes.^{12, 14} Therefore, the purpose of this study was to identify, characterize,
70 and compare the resident progenitor cell populations within the red-red (RR), red-white (RW)
71 and white-white (WW) zones of freshly harvested human cadaver menisci and to characterize
72 the vascularity of human menisci using immunofluorescence and three dimensional (3D)
73 imaging. We hypothesized that microvessels and resident progenitor cells in the inner zone of
74 meniscus would be more prominent than previously reported.

75

76 METHODS

77 *Study Design*

78 The cadaveric studies were conducted according to the approved Institutional Review Board
79 protocol (Pro00052234). Menisci from fresh human cadaveric knees (mean donor age: 21 ± 6.1
80 years) were donated by three tissue banks [Joint Restoration Foundation (JRF, Centennial,
81 CO), Musculoskeletal Transplant Foundation (MTF, Edison, NJ) and Biosource Medical
82 (Lakeland, FL)] for medical research purposes as they were deemed non-compatible with the
83 recipient at the time of matching. Grafts were stored at 4°C at the tissue banks until shipment
84 according to standard procedures and were shipped under sterile conditions on ice, following
85 the same procedure for allografts used in the clinic. Allografts for meniscal transplantation have
86 a 21-day window, thus all donated grafts were between 1 and 21 days post-harvest.¹⁵
87 Specimens were assessed by at least two investigators (initials blinded for review). In our
88 preliminary studies we have determined that the viability of mononuclear cells significantly
89 declined after 7 days post-harvest (*data not shown*), thus grafts greater than 7 days post-
90 harvest were allocated to histological analysis and uDisco experiments, while only fresh grafts
91 were allocated to mononuclear cell isolations and characterization. A total of 34 allografts from

92 17 different donors (including medial and lateral) were used in this study. Tibial plateaus were
93 dissected to harvest medial and lateral menisci along with their entire length preserving 1mm of
94 their peripheral capsular attachments (Fig.1). Fourteen menisci from 7 different donors were
95 used for cell isolation and characterization. Twenty meniscal allografts from 10 different donors
96 were used for assessing vascularity using histology and the modified uDisco 3D staining
97 approach.¹⁶In this work, meniscal zones on cadaveric menisci were identified using the Cooper
98 classification system.¹⁴ For the cell isolation/characterization experiments, zones were identified
99 on cadavers and sectioned, whereas for the 2D/3D immunolabeling experiments meniscal slices
100 were sectioned, imaged as whole slide scans or 3D images and software was used to establish
101 the distance between each zone (Supplementary Fig.1).

102

103 **Mesenchymal Stromal Progenitor Cell Prevalence: Identification, Quantification and** 104 **Characterization**

105 *Cell Isolation from fresh meniscus grafts*

106 The red-red (RR), red-white (RW), and white-white (WW) zones were dissected and sectioned
107 into equal thirds as measured by a caliper from the inner aspect to the marginal border of the
108 meniscus by cutting in the radial direction, to replicate the clinical setting and to aid in a more
109 standardized sectioning technique (Fig. 2A). Sterile gauge was used to remove excess media.
110 Meniscal tissue was then placed in sterile tubes and wet weights were recorded. Tissue was
111 manually minced to ~1mm² pieces in a sterile environment and then enzymatically digested.
112 Since it is well established that meniscus tissue cellular content varies between each zone,^{17, 18}
113 several dissociation procedures were tested and the procedure yielding the highest cellular
114 content for all zones was chosen. Highest yields were obtained from dissociation of meniscus
115 tissue in 0.02% pronase (Millipore, Temecula, CA) for 1h at 37°C, followed by 18h 0.02%
116 collagenase II (LS004205, Worthington Biochemical Corporation) at 37°C¹⁹, therefore this
117 procedure was chosen for meniscal cell content characterizations. Isolated cells were plated in
118 culture-treated plates in approximately 2x10³ cells/cm² density and incubated overnight at 37°C
119 in 5% CO₂. Adherent cells were cultured at 37°C/5% CO₂ in growth medium containing 1mM L-
120 glutamine (Invitrogen, Carlsbad, CA), 1% antibiotic antimycotic solution (Hyclone, Marlborough,
121 MA) in Dulbecco's modified eagle medium (DMEM, GIBCO, Carlsbad, CA) and 10% fetal
122 bovine serum (FBS, Gemini Bioproducts, West Sacramento, CA). Following the
123 recommendations regarding nomenclature and mesenchymal stem/progenitor cell
124 characterization from the International Society for Cell Therapy (ISCT), progenitor cells from the

125 meniscus are referred to as mesenchymal stromal cells and cultured meniscal cells (CMCs) in
126 this manuscript and they are clearly distinguished from Bone Marrow-derived Mesenchymal
127 Stromal Cells (BM-MSCs) that were used as controls for the various *in vitro* assays.^{20, 21} BM-
128 MSC were isolated from human bone marrow aspirate (Lonza, Benicia, CA) as previously
129 described.²²⁻²⁴

130 *Self-Renewal assessment (Colony Forming Unit-Fibroblast Assay)*

131 Self-renewal of cultured meniscus cells (CMCs) was assessed using a standard CFU-F assay
132 as previously described.²⁵ Briefly, cells isolated from different zones of the meniscus were
133 separately plated onto 6-well plates at 10^4 cells/well in culture media, with media changed twice
134 per week. Between 7 and 14 days medium was removed, and cells were washed with PBS.
135 Afterward, cells were fixed with 4% formaldehyde, stained with hematoxylin, and aggregates of
136 50 cells or more were scored as CFUs.

137

138 *Meniscus Stromal Progenitor Cell Characterization and Expansion (Surface markers)*

139 Meniscus stromal cells were characterized immediately after isolation using flow cytometry with
140 antibodies against the following Mesenchymal Stromal Cell (MSC) surface markers: CD105
141 (326-050, Ancell Corporation, Stillwater, MN), CD90 (MCA90F; Biorad, Hercules, CA), CD44
142 (559942; BD Pharmigen, San Diego, CA), CD29 (PB-219-T100; Abcore, Ramona, CA) as well
143 as respective isotype controls.^{20, 21} Afterward, meniscal cells were cultured, split twice when
144 confluence was reached, characterized at passage 2 (P2), and compared to cultured bone
145 marrow-derived MSCs (BM-MSCs, \leq P5, Lonza, Benicia, CA) using the same markers.

146

147 *In vitro Differentiation to Mesenchymal Linages*

148 **Osteogenesis:** For assessment of osteogenic differentiation, CMCs and BM-MSCs at low
149 passage were plated in 24 well plates (6×10^4 per well) in triplicates and cultured in complete
150 high glucose DMEM (Life Technologies). Once confluence was reached, the medium was
151 supplemented with 100nM dexamethasone (D4902, Sigma, St Louis, MO), 10mM β -
152 glycerophosphate (G9422, Sigma) and 50 μ g/ml L-ascorbic acid (A4544, Sigma) for 7 days or 21
153 days, with media changes every other day. Alkaline phosphatase (ALP) activity assay was
154 performed to determine osteogenic differentiation after 7 days according to the manufacturer's
155 protocol (ab83369, Abcam, Cambridge, MA). Production of pNP, was determined by measuring

156 absorbance at 405nm using a microplate reader (Bio-Rad). ALP activity (U/ml) in the test
157 samples was calculated based on the equation: $ALP\ activity = (B/\Delta T * V) * D$, where B = amount
158 of pNP in sample wells calculated from standard curve (μmol). ΔT = reaction time (minutes), V =
159 original sample volume added into the reaction well (mL), and D = sample dilution factor. ALP
160 activity was normalized to total protein content quantified using BCA assay (Promega, San Luis
161 Obispo, CA) performed on parallel wells. Each sample was run in technical triplicates. Lastly,
162 cells were cultured in differentiation media for three weeks and gene expression of osteogenic
163 marker Collagen-1 was evaluated. In order to evaluate osteogenic gene expression, cells were
164 harvested and RNA isolated. For RNA isolation, media were aspirated, and cells lysed with RLT
165 buffer (Qiagen, Valencia, CA) containing β -mercaptoethanol (M3148, Sigma). Lysates were
166 transferred to 1.5 ml tubes and a handheld pestle and mortar was used to fully homogenize the
167 cells in the RLT buffer and RNA was isolated with the RNeasy mini kit (Qiagen) following the
168 manufacturer's recommendations. RNA yields were determined spectrophotometrically using a
169 Nanodrop system (Thermofisher, Waltham, MA), and RNA was reverse-transcribed using the
170 high-capacity cDNA reverse transcription kit (Applied Biosystems, Thermofisher). Gene
171 expression analysis was conducted using Taqman gene expression assay for Collagen-1
172 (Hs00164004_m1, Thermofisher). Target gene mRNA levels were quantified using FAM-MBG
173 technology (Bio-RAD). The threshold cycle (Ct) value of 18S rRNA was used as an internal
174 control using the Taqman gene expression FAM/MGB probe system (4333760F, Thermofisher).
175 The Livak method was used to calculate $\Delta\Delta C_t$ values and fold change was calculated as $2^{-\Delta\Delta C_t}$
176 as previously described.²⁶

177 **Adipogenesis:** For assessment of adipogenic potential, CMCs and BM-MSCs at low passage
178 were plated in 24 well plates (6×10^4 cells per well) in triplicates and cultured in complete high
179 glucose DMEM (Life Technologies) until they were fully confluent. Adipogenic differentiation was
180 induced as previously described.^{27, 28} Briefly, medium was changed to "induction medium"
181 composed of complete high glucose DMEM and supplemented with $1\mu\text{M}$ dexamethasone
182 (D4902, Sigma), $10\mu\text{M}$ insulin (I6634, Sigma), 0.5mM 3-isobutyl-1-methylxanthine (IBMX, I7018,
183 Sigma) and $200\mu\text{M}$ indomethacin (I8280, Sigma) for three days, followed by 2-3 days of
184 "maintenance medium", composed of complete high glucose DMEM and $10\mu\text{M}$ insulin. Cells
185 were inspected daily for presence of adipogenic vacuoles. Five full cycles of induction followed
186 by maintenance were performed. Finally, wells were fixed in ice-cold formalin and washed and
187 stained with Oil-Red-O (O0625, Sigma) for 15 minutes. Cells were then washed three times with
188 double distilled water and microphotographs were taken at 20x magnification using an EVOS XL
189 Core imaging system (Thermo scientific).

190 **Chondrogenesis:** The chondrogenic potential of CMCs was assessed as previously
191 described.²⁷ Cells were trypsinized, neutralized with serum-containing low glucose DMEM and
192 counted. Cell aliquots of 5×10^5 meniscal cells or BM-MSCs at low passage were span at 240g
193 for 5min and all media carefully removed. Pellets were resuspended in serum-free low glucose
194 media and span again at 240g for 5min to ensure complete removal of serum-containing
195 medium. Then, cells were resuspended in 100 μ l chondrogenic differentiation medium composed
196 of low glucose DMEM, 1xITS (I2521, Sigma), 0.1 μ M dexamethasone (D4902, Sigma), 40 μ g/ml
197 proline (Sigma), 50 μ g/ml ascorbic acid (Sigma) and 10ng/ml TGF β 1 (240B002, R&D Systems,
198 Minneapolis, MN). The 100 μ l cell suspension was placed in transwells in order to induce disc-
199 shaped 3D formation. The transwell plate was centrifuged at 200g for 5 minutes, and then filter
200 inserts were transferred into a 24-well plate containing differentiation medium. Chondrogenic
201 media were changed every two days. After 21 days, discs were fixed in formalin for 1 hour and
202 dehydrated in passing through an increasing-grade series of ethanol baths. Afterward, discs
203 were embedded in paraffin blocks, cut into 5 μ m sections and stained with Alcian Blue to identify
204 chondrocytes. Whole slide scans were attained and imaged using QuPath software.

205

206 ***Vascularity Assessment using standard histology, immunofluorescent labeling and 3D***
207 ***imaging***

208 *Vascular Tree Histology*

209 Samples were fixed in 10% buffered formalin. Following fixation, samples were dehydrated by
210 passing through an increasing-grade series of ethanol baths, paraffin embedded, sectioned
211 (4 μ m thick), deparaffinized and histological stains performed according to standard procedures.
212 Hematoxylin and Eosin (H&E) staining was used for morphological evaluation. Masson's
213 trichrome (MTC) stain was performed to further evaluate structure of the extracellular matrix and
214 visualization of the larger vessels. QuPath quantitative pathology and image analysis software
215 was used for imaging H&E and MTC full slide scans as well as quantifying the distance between
216 zones.

217

218 *Characterization of Microvasculature via Immunofluorescence*

219 Immunofluorescence was performed on formalin-fixed (7 days in formalin), paraffin-embedded
220 tissue sections. Briefly, sections were deparaffinized, rehydrated in PBS with 0.025% Triton-X
221 (PBS-T), treated with antigen retrieval solution at 98°C for 1hr (pH 6.1; Dako #S1699, Agilent

222 Technologies, Carpinteria, CA) and blocked with 10% normal donkey serum in PBS-T.
223 Endothelial cells were detected on meniscus cross sections by CD31 (1:50 dilution; ab28364,
224 Abcam), α SMA (1:250 dilution, Abcam, Cat# ab21027) and Alexa488-conjugated lectin antibody
225 (1:200 dilution, Dylight, Cat# DL-1174, Vector Labs, Burlingame, CA) in blocking solution,
226 overnight at 4°C. To control for unspecific background labeling, primary antibody was omitted on
227 background labeling controls. Then, sections were washed three times in PBS-T, followed by
228 incubation with Cy5 (donkey anti-rabbit), Cy3 (donkey anti-goat) secondary antibody (1:200
229 dilutions, all from Jackson ImmunoResearch, Westgrove, PA) for 2 hours at room temperature.
230 Subsequently, sections were washed three times in PBS-T and mounted with Prolong Gold with
231 DAPI (Life Technologies, Carlsbad, CA). Vascularity was assessed stereologically based on the
232 morphology and topology of endothelial cell arrangement in the tissue. Vessels were considered
233 structures with lumen and colocalization of all vascular markers. Microvessels with one to three
234 endothelial cells (CD31-positive cells) spanning the vessel circumference were classified as
235 capillaries as previously described.²⁹ Whole slide scans were taken using a Leica DMI8
236 fluorescence microscope and imaged using Imaris Core 9.3 (Oxford Instruments, Concord, MA).
237 Higher magnification images (40x) of selected areas were taken with a Nikon Eclipse Ti-2
238 fluorescence microscope (Melville, NY).

239

240 *Qualitative Three-Dimensional Imaging using Light Sheet Microscopy*

241 Meniscal allografts from cadavers were fixed in formalin. Meniscus tissue was cleared using a
242 modified uDisco passive clearing and staining procedure for whole organs.¹⁶ This multi-step
243 procedure allows for staining of entire pieces of tissue (or whole organs) with antibodies without
244 the requirement for sectioning of the tissues. Tissues are made fully transparent, labeled using
245 the same antibodies required for immunofluorescence and then imaged using light sheet laser
246 fluorescence microscopy. The ultimate 3D imaging of solvent-cleared organs (uDisco) protocol
247 previously published in mice¹⁶ was optimized and adjusted for human cadaveric menisci.
248 Meniscus tissue was segmented into quarters and 2mm thin slices and fixed in formalin for up to
249 four weeks, similar to the procedure followed in mouse tissues. Then tissue was incubated for 1
250 week in wash/permeabilization solution (0.4% v/v Triton-X, 0.3M glycine w/v, 20% DMSO v/v all
251 from Sigma), followed by 8 days in primary antibody (anti-CD31, 1:50 dilution; ab28364, Abcam)
252 diluted in wash/permeabilization solution at 37°C. Tissue was washed overnight with
253 permeabilization solution and incubated for 6 days with secondary antibody (Alexa Fluor[®] 488-
254 conjugated AffiniPure Donkey Anti-Rabbit IgG secondary antibody; Jackson Immunoresearch),

255 followed by a second wash with permeabilization solution, 37°C. Afterward, all cells were
256 labeled with TO-PRO[®]-3 nuclear stain (0.1% v/v, Thermofisher Scientific) for 4 days at 4°C.^{30, 31}
257 and gradient dehydrated in *tert*-butanol (Sigma, 360538). Specifically, tissue pieces were
258 incubated in ascending grades of *tert*-butanol solution diluted in distilled water (30%, 50%, 70%,
259 90% and 96%) for 1-3 days each and 100% *tert*-butanol at 37°C in the dark for 1 day,
260 delipidated using dichloromethane (DCM, Sigma, 270997) for one day, and finally cleared with
261 dibenzyl ether (DBE) at RT in the dark for at least 3 days. A lightsheet fluorescent microscope
262 (LaVision Biotec Ultravision II, Miltenyi Biotec, Auburn, CA) was used for imaging and Imaris 9.3
263 was used for 3D reconstruction of the acquired images.

264 *Statistical Analyses*

265 All data are presented as mean \pm standard deviation unless otherwise stated. Non-repeated
266 measures analysis of variance and Tukey–Kramer post hoc analysis were performed on sample
267 means for each analysis. For the changes in gene expression following three weeks of
268 osteogenic induction one-way ANOVA was performed using Sidak post hoc analysis for multiple
269 comparisons between the induced and non-induced controls of each group (BM-MSCs, RR,
270 RW, and WW respectively). For flow cytometry marker analysis, two-way ANOVA was
271 performed using Dunnett’s post hoc analysis for comparisons between markers detected in
272 different zones, using the WW zone as the control group. Statistical significance was set at
273 $p < 0.05$. GraphPad Prism 8 software (Irvine, CA) was used to analyze the data.

274

275 **RESULTS**

276 ***PROGENITOR CELL PREVALENCE***

277 ***Cell Isolation from meniscal grafts, cell yields and self-renewal potential in vitro***

278 The enzymatic digestion protocol produced comparable results between medial or lateral
279 menisci in all three zones (n=6 donors, $p > 0.05$; Figure 2B). Therefore, data from medial and
280 lateral menisci were pooled and analyzed per zone. Clonogenic potential of isolated cells from
281 each zone was confirmed using low CFU-F assay. Colony counts showed that freshly isolated
282 cells were clonogenic in culture. Further, there were no significant differences in clonogenicity of
283 the cells isolated from the three meniscal zones ($p > 0.05$, Figure 2C).

284

285 ***Phenotypic analysis; Cell surface marker expression and assessment of differentiation***
286 ***potential in vitro***

287 Flow cytometry analysis of cells from the three meniscal zones displayed presence of two
288 distinct subpopulations of cells immediately after isolation. One subpopulation was
289 CD44⁺CD105⁺CD29⁺CD90⁺ and the other one was CD44⁻CD105⁻CD29⁻CD90⁻ (Figure 3A top
290 panel). Additionally, flow cytometry of cultured meniscus cells (CMC) at passage 2 displayed a
291 shift of all four markers expression to the right (Figure 3A, bottom panel). Surface marker
292 expression analysis showed differential marker expression patterns between different zones
293 (Figure 3B). The WW zone contained a larger proportion of cells that express all four MSC
294 markers (45.07±20.36%) compared to RR and RW zones (17.75 ±10.17 % and 23.47±13.62 %
295 respectively p<0.05, Figure 3C).

296 CMCs were induced toward the three mesenchymal lineages (osteogenic, chondrogenic, and
297 adipogenic) commonly used to assess MSC stem/progenitor cell potential.^{20, 21} After one week
298 of induction with osteogenic media, CMCs from all zones displayed increased ALP activity
299 compared to non-induced respective controls (Figure 4A). ALP activity of BM-MSCs that were
300 treated under the same conditions were significantly higher (p<0.05), although after three weeks
301 of osteogenic induction all groups displayed increased Collagen type I expression similar to BM-
302 MSCs (p>0.05 between groups, Figure 4B). CMCs from all zones were successfully induced
303 towards the adipogenic lineage after 5 weeks of induction. CMCs from the RR-zone displayed
304 higher prevalence of fully developed adipocytes with lipid droplets similar to those observed in
305 induced BM-MSCs under the same conditions. CMCs from all zones were successfully induced
306 to the chondrogenic lineage after 3 weeks in 3D culture in transwells, even though RW pellets
307 showed less chondrogenic differentiation potential compared to BM-MSCs controls as can be
308 observed in less Alcian Blue-stained extracellular matrix (Figure 4C).

309

310 ***VASCULARITY ANALYSIS***

311 ***Histologic features and triple immunofluorescence colocalization analysis***

312 Histological analysis and standard H&E staining confirmed the presence of larger vessels in the
313 RR and RW zones (Figure 5A-B). Masson's Trichrome staining, which can differentiate between
314 smooth muscle and extracellular matrix, confirmed the presence of a network of arteries and
315 veins in the RR and RW zones (Figure 5B). H&E and Masson's Trichrome staining utilize dyes
316 to differentiate between cellular structures based on their generic physicochemical properties

317 but cannot detect finer elements within a tissue including individual cells or smaller vessels,
318 such as capillaries, that are composed of a single layer of endothelial cells and do not possess
319 a smooth muscle actin lining (Figure 5C). Therefore, a more detailed immunofluorescence
320 analysis was employed, which uses antibodies that detect specific antigens within the tissue of
321 interest. To this end, triple immunostaining with α SMA and endothelial markers CD31 and lectin
322 revealed the presence of endothelial cells in all three zones, including the WW zone, especially
323 closer to the perimeter of the meniscus (Figure 6). The scan of entire IF-stained slides showed
324 that when dividing the meniscus into three zones using the most conservative approach, that is
325 $\leq 1/3$ of total area, blood vessels were found in the WW zone. (Supplemental Figure 1 presents
326 the full slide scan of the images shown in Figure 6).

327

328 ***Three-dimensional Imaging of Vessels in the Meniscus***

329 CD31⁺ staining demonstrated presence of endothelial cells, visualizing the vascular tree in RR
330 towards RW and positive colocalization of green and red staining in the WW zone, especially on
331 the periphery of the meniscus, confirming the findings in 2D immunofluorescence (Figure 7 and
332 Supplementary Video 1).

333

334 **DISCUSSION**

335 **The main finding of this study was that multipotent mesenchymal stromal progenitor cells and**
336 **blood vessels were observed in all three zones of the meniscus including the WW zone.**

337 Isolated meniscus cells were clonogenic *in vitro* with no significant differences in the self-
338 renewal potential between the three meniscal zones. Flow cytometry analysis demonstrated that
339 these progenitor cells were expressing consensus MSC surface markers (CD44, CD105, CD29
340 and CD90). Meniscus stromal progenitor cells were enriched after *in vitro* culture, due to the
341 plastic adherence that filters out non-adherent cells. Lastly, CMCs from all three meniscal zones
342 were able to successfully differentiate into the three mesenchymal lineages (osteogenic,
343 adipogenic and chondrogenic), and found slightly inferior to BM-MSCs in their osteogenic and
344 adipogenic potential. Bigger vessels were observed in the RR and RW zones, and smaller
345 vessels were identified in the WW zone using 2D immunofluorescence co-localization of
346 endothelial markers and alpha smooth muscle actin in combination with a modified uDISCO 3D
347 imaging approach.

348 Biologic augmentation approaches are currently being investigated to promote chemotaxis,
349 cellular proliferation, and/or matrix production at the site of meniscal repair. These approaches
350 include mechanical stimulation, marrow venting procedures, fibrin clots, injection of platelet-rich
351 plasma, and stem cell-based therapies that involve injection of autologous MSCs.^{32, 33} These
352 approaches may augment an inherent meniscus healing capacity if resident progenitor/stem
353 cells are present, as demonstrated in rabbits and humans.^{9, 34, 35} The main role of resident
354 mesenchymal progenitor cells in connective tissues is to maintain homeostasis and contribute to
355 tissue repair when needed.³⁶ Hennerbichler *et al* demonstrated that punch defects directly filled
356 with the removed punches, showed no significant difference in healing potential between the
357 vascularized and avascular meniscus zone.³⁷ Furthermore, Croutze *et al* reported equivalent
358 differentiation potential toward chondrogenic phenotype and extracellular matrix production of
359 human meniscus cells isolated from the inner and outer zones.³⁸ Mauck *et al* reported similar
360 differentiation potential of cells isolated from different zones of calf meniscus.¹⁰

361 Mesenchymal stromal cells (MSCs) are a heterogeneous cell population that consists of a
362 mixture of multipotent and more committed progenitors. MSCs isolated from the bone marrow
363 (BM-MSCs) have been shown to comply to the established stem cell criteria, that is they are
364 multipotent, clonogenic *in vitro* and able to produce skeletal tissues via serial transplantations *in*
365 *vivo*.²⁵ Stromal mesenchymal progenitors are found in multiple other tissues (adipose tissue,
366 umbilical cord, etc), are clonogenic in culture, can be induced to differentiate into multiple
367 lineages *in vitro* beyond skeletal tissues and express similar markers with BM-MSCs.²⁵ Both
368 terms are sometimes used interchangeably in the literature, resulting in ISCT issuing a set of
369 criteria in a position statement to assist comparisons between different studies.^{20, 21} Based on
370 ISCT criteria for mesenchymal stromal progenitor identification, we characterized CMCs on the
371 basis of positive selection using plastic adherence and multipotentiality. We also assessed the
372 expression of MSC consensus markers and compared them to freshly isolated and cultured BM-
373 MSCs.

374 It is known that the cells of the meniscus differ in their morphology and their *in vitro* properties
375 depending on their location.¹² At least four different meniscus cell types have been identified in
376 the rabbit meniscus using fluorescent and scanning electron microscopy imaging.¹⁸ In the
377 present study we demonstrated a higher prevalence of isolated CD44⁺CD105⁺CD29⁺CD90⁺
378 meniscus cells in the WW zone compared to the other zones. Surface marker expression of
379 cells freshly isolated from the WW zone was significantly greater than from the other two zones
380 using standard flow cytometry analysis. The higher proportion of CD44⁺CD105⁺CD29⁺CD90⁺

381 cells in the WW zone suggests that the WW zone hosts a more homogeneous progenitor
382 population compared to the other zones as defined by expression of those four markers, CFU-F
383 clonogenicity and positive selection through plastic adherence. Interestingly, our results
384 demonstrate that cells isolated from the RR zone have similar potential to be induced to the
385 adipogenic lineage as BM-MSCs, whereas the cells from RW and WW could not be efficiently
386 induced towards the adipogenic phenotype *in vitro*. Additionally, RW cells might not be as
387 potent towards induction to the chondrogenic phenotype compared to RR and WW. This
388 suggests that some of the cells in the RW and WW zones cannot differentiate towards the
389 chondrogenic adipogenic lineages, so they are more specialized toward the fibrocartilage
390 phenotype of the meniscus. However, the presence of other cell types in the RR as well as the
391 plasticity of the resident CD44⁺CD105⁺CD29⁺CD90⁺ CMCs identified in RR zone might be an
392 important factor that contributes to the regenerative potential of that zone.⁸ Future research is
393 needed to determine whether this phenomenon is age-dependent or related to other factors. It is
394 unknown if the sole presence of progenitor cells can facilitate improved healing and therefore
395 future studies are warranted. Also, recruitment mechanisms of these cells to the injury site
396 needs to be addressed using *in vivo* models. Vascularization and progenitor cell availability will
397 play an important role in recruitment of the cells and their contribution to the healing process.

398 Tears in the avascular zone have historically been treated with debridement, given the lower
399 likelihood of successful healing of a repair in avascular tissue.³⁹ Although repair of meniscal
400 tears in the avascular white-white zone have recently been reported to yield satisfactory
401 outcomes.^{40, 41} Cinque *et al.* reported low meniscal repair failure rates in avascular zone with
402 only 3% of patients requiring a second surgery for a failed meniscus repair.⁴² Noyes *et al.*⁴³
403 reported that 62% of red-white zone inside-out meniscal repairs had normal or nearly normal
404 characteristics for pain, swelling, jumping and their Cincinnati score. In theory, meniscal tears
405 require vascularization to deliver the biologic factors necessary for tissue repair. However, some
406 animal studies demonstrate that meniscal tissue may heal without significant vascular
407 contributions.^{37, 44} In the present study, following identification of primary tissue features with
408 standard histology (H&E and MTC stains), a comprehensive combined 2D and 3D
409 immunofluorescence analysis was used to define vessels using cytological features and identify
410 the presence of vessel-specific markers in cadaveric menisci. H&E and MTC staining revealed
411 larger vessels in the RR zone of meniscus spanning towards the RW zone and sprouting to
412 smaller arterioles. Small vessels and endothelial cells were found also in the WW zone, mainly
413 in the periphery, suggesting that the WW zone might not be completely devoid of vasculature.
414 However, it is possible that these are remnants of previously vascularized fetal tissues that

415 regressed after birth, as has been shown previously.¹⁴ Thus, further research using functional
416 imaging *in vivo* or cell tracking in animal models is needed to determine whether there is
417 functional vasculature in the WW zone.^{45, 46}

418 Large blood vessels were not found within the WW zone. However, around the perimeter of the
419 tissue small vessels and endothelial cells were spotted, suggesting that they might be part of
420 microvessels or remnants from vasculature that regressed in adulthood and that could
421 potentially be revived with appropriate angiogenic stimulation. Schrepfer *et al.* reported that
422 MSCs injected into the lungs get trapped in the pulmonary capillary network because their mean
423 size is greater than the pulmonary capillary lumen.⁴⁷ The use of vasodilation agents has been
424 proposed in combination with such treatments to improve perfusion and stem cell migration.⁴⁷
425 Importantly, recent evidence suggests that vasculature could increase in the case of meniscal
426 tears, upregulating angiogenic factors, such as vascular endothelial growth factor (VEGF).⁴⁸
427 This could modify the affluence of progenitor cells not only by chemotaxis but as a *de novo*
428 source of pericytes.⁴⁹ The specific topology of the capillary network in the WW zone of healthy
429 adult donors is yet to be mapped. The vessel distribution may be affected by age, health or
430 fitness level, and other factors that are yet to be determined. In this study we demonstrate that
431 there is a small amount of vasculature and a significant population of progenitor cells in the WW
432 zone of the meniscus. Future studies that investigate the healing potential of these resident
433 stem/progenitor cells are warranted.

434

435

436 **Limitations**

437 This study is not without limitations. The sample size was limited and both medial and lateral
438 meniscus were included. The donated cadaveric menisci were never frozen (received within 21
439 days) and stored at 4°C increasing the potential of cell death immediately post-harvest
440 compared to the *in vivo* setting. The mean age of the specimens was 21 years old, which is not
441 representative of an older population. Thus, further studies exploring the cellular content and
442 vascularity of the older population is warranted. Only three zones were selected for the
443 analysis: inner, middle and marginal, each representing a third of the width of the tissue which
444 might not represent a true division of the vascular tree density throughout the meniscus tissue.
445 Vessel distribution might be different between medial and lateral menisci and could also be
446 affected by age and/or health status. It is known that in every cell isolation procedure from a

447 tissue cell yields inherently vary. Since the cellular composition of meniscus is heterogeneous,
448 the current cell isolation approach was optimized for our work because it was shown as the
449 most efficient for all three zones for our grafts. Additionally, no significant differences were
450 observed between medial and lateral menisci. However, it might not be pertinent for grafts with
451 different characteristics, such as fetal and/or neonatal menisci, or menisci from aged and
452 diseased populations. Finally, the presence of blood vessels does not necessarily indicate
453 functional vascularization, which requires further analysis. These vessels might be remnants of
454 retreating vasculature from the fetal meniscus.

455

456 **CONCLUSIONS**

457 In conclusion, our results demonstrate the presence of resident mesenchymal progenitors in all
458 three meniscal zones of healthy adult donors without injury. Additionally, our results
459 demonstrate the presence of vascularization in the WW zone.

460

461 **Figure Legends**

462 **Figure 1. Research Design.** (1) The first aim of this study was to characterize and identify the
463 resident stromal progenitor cell population in all three zones in freshly harvested human
464 cadaveric menisci. (2) The second aim was to characterize the vascularity of the menisci, using
465 histology, immunofluorescence (IF), and three-dimensional (3D) light sheet fluorescence
466 microscopy.

467 **Figure 2. Evidence of resident stromal progenitor cells in the WW of human meniscus.**
468 (A) Dissection of meniscal zones for cell isolation. (B) Box and Whisker plots of cell yields of
469 medial or lateral menisci normalized to tissue wet weight. Lines display median values. (C)
470 Colony formation of isolated cells in vitro. Meniscal cells from all zones were clonogenic in
471 culture. No significant differences were found between zones when assessed by CFU-assays
472 ($p>0.05$).

473 **Figure 3. Identification of freshly isolated meniscus cells vs. cultured controls using flow**
474 **cytometry** (A) Flow cytometry analysis of cells from the three meniscal zones displayed
475 presence of two distinct subpopulations of cells immediately after isolation (top panel). One
476 subpopulation was positive to MSC surface markers and the other population was negative.
477 Meniscal cells that were selected using plastic adherence and cultured to P2 were all positive

478 for all MSC markers similarly to BM-MSCs (bottom panel). **(B)** Quantification of individual cell
479 surface markers showing the proportion of each marker per zone. All four markers showed
480 higher expression in the WW zone compared to RR and RW ($p < 0.05$). **(C)** Proportion of
481 $CD105^+CD44^+CD29^+CD90^+$ cells per zone, $p < 0.05$.

482 **Figure 4. Multilineage differentiation potential of meniscal stromal cells.** **(A).** ALP activity
483 after 1 week of osteogenic induction. Controls were cultured for one week without osteogenic
484 media ($*p < 0.05$, $***p < 0.001$) **(B).** Col1 expression after 3 weeks of osteogenic induction
485 ($p < 0.05$). **(C)** . Adipogenesis was induced for 5 weeks with adipogenic supplements. BM-MSCs
486 were treated under the same conditions and were used as assay positive controls. Red-Oil O
487 stains lipid droplets in red. Bars represent 50 μm **(D).** Chondrogenesis was induced in
488 transwells for 3 weeks resulting in disk formation. Disks were processed histologically,
489 sectioned and whole slide scans attained. Alcian blue was used to determine presence of
490 proteoglycans in the disks. BM-MSCs were treated under the same conditions and were used
491 as assay controls. Bars represent 50 μm .

492 **Figure 5. Limitations of simple 2D histology approaches to visualize the vasculature of**
493 **the human meniscus.** **(A):** Schematic Illustration of the three meniscal zones: red-red (RR),
494 red-white (RW), white-white (WW). **(B):** Full thickness cut of the meniscus stained with
495 Hematoxylin & Eosin (H&E) [left] and Masson's Trichome stain [right], and higher magnification
496 (bottom panels) of boxed areas shows relatively low cellularity throughout the RW and WW
497 zones. Top bars represent 1mm, in bottom panels bars represent 100 μm .

498 **Figure 6. Immunofluorescent triple staining with lectin (green), CD31 (orange), α SMA**
499 **(magenta) and DAPI (blue) in all three zones using fluorescent microscopy and imaging with**
500 **two different microscopes. Left images from whole-slide scans were taken (20x scan, Leica).**
501 **Right, orange boxes from left images were identified using a Nikon Eclipse microscope and**
502 **imaged at higher magnification (40x). Whole-slide scans allow visualization of the exact region**
503 **imaged (left images, top right; yellow arrows). Areas were assessed using Qupath software to**
504 **accurately quantify the distances between regions. The RW snapshot shown is at the bottom**
505 **border of the RW zone of the whole-slide scan and was chosen in order to show the continuity**
506 **of the scan. Bigger vessels with α SMA lining and lectin/CD31 can be found in both RR and RW**
507 **zones. However, in WW zone only lectin/CD31/DAPI positive staining was found, suggesting**
508 **presence of relatively smaller vessels, such as capillaries in this area. RR red-red zone; RW,**
509 **red-white zone; WW, white-white zone. Scales bars represent 50 μm .**

510 **Figure 7. Successful clearing of human meniscus with modified uDISCO procedure and**
511 **nucleic staining with To-Pro[®]-3 and the endothelial marker CD31. (A).** Fully transparent
512 slices of human meniscal tissue cleared with a modified uDisco approach. On the left a quarter
513 of fully cleared meniscus. On the right, a slice before and after clearing **(B)**. 2D slice of cleared
514 meniscus tissue stained with only with TO-Pro[®]-3, displaying cells distributed in all 3 zones **(C)**.
515 Three-dimensional reconstruction of meniscus slices after imaging with light sheet fluorescence
516 microscopy. Double-labeling with To-Pro[®]-3 (red, pan-nuclei marker) and CD-31 (green,
517 endothelial marker) indicates presence of vessels of various sizes in all zones. Bigger vessels
518 were found spanning the RR to RW zones, confirming 2D results. Blood Vessels are present in
519 the WW zone. Upper and bottom panels display different views of the same slice. Left; merged
520 channels (red and green), middle; red channel (To-Pro[®]-3), right; green channel (CD31). Arrows
521 point to vessels. Bar represents 500µm.

522

523 **Supplementary Figure 1.**

524 Full slide scans of the same block of meniscus tissue. A. H&E, B. MTC, C, IF staining against
525 lectin, CD31, aSMA. QuPath and Imaris software programs were used to measure and classify
526 the three meniscus regions using the most conservative approach, that is $\leq 1/3$ of long axis
527 (distance is displayed in the image).⁵⁰ The presence of smaller vessels in WW is evident.

528

529 **Supplemental Video**

530 Mp4 video created using Imaris 3D reconstruction software of a meniscus thin section stained
531 with To-Pro[®]-3 and the endothelial marker CD31.

532

533

534 **References**

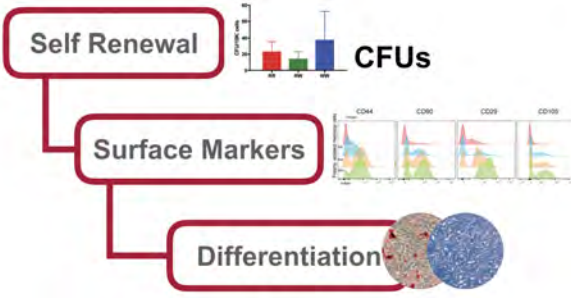
- 535 1. Arnoczky SP, Warren RF. The microvasculature of the meniscus and its response to
536 injury. An experimental study in the dog. *Am J Sports Med.* 1983;11:131-141.
- 537 2. Chahla J, Cinque ME, Godin JA, et al. Meniscectomy and Resultant Articular Cartilage
538 Lesions of the Knee Among Prospective National Football League Players: An Imaging
539 and Performance Analysis. *Am J Sports Med.* 2018;46:200-207.
- 540 3. Dave LY, Caborn DN. Outside-in meniscus repair: the last 25 years. *Sports Med.*
541 *Arthrosc.* 2012;20:77-85.
- 542 4. Stein T, Mehling AP, Welsch F, von Eisenhart-Rothe R, Jäger A. Long-term outcome
543 after arthroscopic meniscal repair versus arthroscopic partial meniscectomy for traumatic
544 meniscal tears. *The American journal of sports medicine.* 2010;38:1542-1548.
- 545 5. Rodeo SA, Monibi F, Dehghani B, Maher S. Biological and mechanical predictors of
546 meniscus function: Basic science to clinical translation. *Journal of Orthopaedic*
547 *Research®.* 2020;38:937-945.
- 548 6. Murakami T, Otsuki S, Okamoto Y, et al. Hyaluronic acid promotes proliferation and
549 migration of human meniscus cells via a CD44-dependent mechanism. *Connect Tissue*
550 *Res.* 2019;60:117-127.
- 551 7. Tarafder S, Gulko J, Sim KH, Yang J, Cook JL, Lee CH. Engineered Healing of
552 Avascular Meniscus Tears by Stem Cell Recruitment. *Sci Rep.* 2018;8:8150.
- 553 8. Kobayashi K, Fujimoto E, Deie M, Sumen Y, Ikuta Y, Ochi M. Regional differences in the
554 healing potential of the meniscus—an organ culture model to eliminate the influence of
555 microvasculature and the synovium. *The Knee.* 2004;11:271-278.
- 556 9. Shen W, Chen J, Zhu T, et al. Intra-articular injection of human meniscus
557 stem/progenitor cells promotes meniscus regeneration and ameliorates osteoarthritis
558 through stromal cell-derived factor-1/CXCR4-mediated homing. *Stem cells translational*
559 *medicine.* 2014;3:387-394.
- 560 10. Mauck RL, Martinez-Diaz GJ, Yuan X, Tuan RS. Regional multilineage differentiation
561 potential of meniscal fibrochondrocytes: implications for meniscus repair. *Anat Rec*
562 *(Hoboken).* 2007;290:48-58.
- 563 11. Humphrey JD, Dufresne ER, Schwartz MA. Mechanotransduction and extracellular
564 matrix homeostasis. *Nature reviews Molecular cell biology.* 2014;15:802-812.
- 565 12. Athanasiou KA, Sanchez-Adams J. Engineering the knee meniscus. *Synthesis Lectures*
566 *on Tissue Engineering.* 2009;1:1-97.
- 567 13. KING D. THE HEALING OF SEMILUNAR CARTILAGES. *JBJS.* 1936;18:333-342.
- 568 14. Karia M, Ghaly Y, Al-Hadithy N, Mordecai S, Gupte C. Current concepts in the
569 techniques, indications and outcomes of meniscal repairs. *European Journal of*
570 *Orthopaedic Surgery & Traumatology.* 2019;29:509-520.
- 571 15. Verdonk R, Kohn D. Harvest and conservation of meniscal allografts. *Scand J Med Sci*
572 *Sports.* 1999;9:158-159.
- 573 16. Pan C, Cai R, Quacquarelli FP, et al. Shrinkage-mediated imaging of entire organs and
574 organisms using uDISCO. *Nat Methods.* 2016;13:859-867.
- 575 17. Grogan SP, Duffy SF, Pauli C, Lotz MK, D'Lima DD. Gene expression profiles of the
576 meniscus avascular phenotype: A guide for meniscus tissue engineering. *Journal of*
577 *Orthopaedic Research®.* 2018;36:1947-1958.
- 578 18. LE GRAVERAND M-PH, Ou Y, Schield-Yee T, et al. The cells of the rabbit meniscus:
579 their arrangement, interrelationship, morphological variations and cytoarchitecture. *The*
580 *Journal of Anatomy.* 2000;198:525-535.
- 581 19. Sanchez-Adams J, Athanasiou KA. Regional effects of enzymatic digestion on knee
582 meniscus cell yield and phenotype for tissue engineering. *Tissue Eng Part C Methods.*
583 2012;18:235-243.

- 584 **20.** Horwitz E, Le Blanc K, Dominici M, et al. Clarification of the nomenclature for MSC: The
585 International Society for Cellular Therapy position statement. *Cytotherapy*. 2005;7:393-
586 395.
- 587 **21.** Dominici M, Le Blanc K, Mueller I, et al. Minimal criteria for defining multipotent
588 mesenchymal stromal cells. The International Society for Cellular Therapy position
589 statement. *Cytotherapy*. 2006;8:315-317.
- 590 **22.** Sheyn D, Shapiro G, Tawackoli W, et al. PTH Induces Systemically Administered
591 Mesenchymal Stem Cells to Migrate to and Regenerate Spine Injuries. *Mol Ther*.
592 2016;24:318-330.
- 593 **23.** Sheyn D, Ben-David S, Shapiro G, et al. Human Induced Pluripotent Stem Cells
594 Differentiate Into Functional Mesenchymal Stem Cells and Repair Bone Defects. *Stem*
595 *cells translational medicine*. 2016;5:1447-1460.
- 596 **24.** Sheyn D, Pelled G, Netanel D, Domany E, Gazit D. The effect of simulated microgravity
597 on human mesenchymal stem cells cultured in an osteogenic differentiation system: a
598 bioinformatics study. *Tissue Eng Part A*. 2010;16:3403-3412.
- 599 **25.** Wilson A, Webster A, Genever P. Nomenclature and heterogeneity: consequences for
600 the use of mesenchymal stem cells in regenerative medicine. *Regenerative medicine*.
601 2019;14:595-611.
- 602 **26.** Schmittgen TD, Livak KJ. Analyzing real-time PCR data by the comparative C T method.
603 *Nature protocols*. 2008;3:1101.
- 604 **27.** Mizrahi O, Sheyn D, Tawackoli W, et al. Nucleus pulposus degeneration alters
605 properties of resident progenitor cells. *Spine J*. 2013;13:803-814.
- 606 **28.** Sheyn D, Ben-David S, Shapiro G, et al. Human iPSCs Differentiate Into Functional
607 MSCs and Repair Bone Defects. *Stem Cells Transl Med*. 2016.
- 608 **29.** Waring CD, Vicinanza C, Papalamprou A, et al. The adult heart responds to increased
609 workload with physiologic hypertrophy, cardiac stem cell activation, and new myocyte
610 formation. *Eur Heart J*. 2014;35:2722-2731.
- 611 **30.** Nehrhoff I, Ripoll J, Samaniego R, Desco M, Gomez-Gavero MV. Looking inside the
612 heart: a see-through view of the vascular tree. *Biomed Opt Express*. 2017;8:3110-3118.
- 613 **31.** Song E, Seo H, Choe K, et al. Optical clearing based cellular-level 3D visualization of
614 intact lymph node cortex. *Biomed Opt Express*. 2015;6:4154-4164.
- 615 **32.** Murrell WD, Anz AW, Badsha H, Bennett WF, Boykin RE, Caplan AI. Regenerative
616 treatments to enhance orthopedic surgical outcome. *PM&R*. 2015;7:S41-S52.
- 617 **33.** Woodmass JM, LaPrade RF, Sgaglione NA, Nakamura N, Krych AJ. Meniscal repair:
618 reconsidering indications, techniques, and biologic augmentation. *JBJS*. 2017;99:1222-
619 1231.
- 620 **34.** Segawa Y, Muneta T, Makino H, et al. Mesenchymal stem cells derived from synovium,
621 meniscus, anterior cruciate ligament, and articular chondrocytes share similar gene
622 expression profiles. *Journal of Orthopaedic Research*. 2009;27:435-441.
- 623 **35.** Shen W, Chen J, Zhu T, et al. Osteoarthritis prevention through meniscal regeneration
624 induced by intra-articular injection of meniscus stem cells. *Stem cells and development*.
625 2013;22:2071-2082.
- 626 **36.** Mabuchi Y, Matsuzaki Y. Prospective isolation of resident adult human mesenchymal
627 stem cell population from multiple organs. *Int J Hematol*. 2016;103:138-144.
- 628 **37.** Hennerbichler A, Moutos FT, Hennerbichler D, Weinberg JB, Guilak F. Repair Response
629 of the Inner and Outer Regions of the Porcine Meniscus in Vitro. *The American Journal*
630 *of Sports Medicine*. 2007;35:754-762.
- 631 **38.** Croutze R, Jomha N, Uludag H, Adesida A. Matrix forming characteristics of inner and
632 outer human meniscus cells on 3D collagen scaffolds under normal and low oxygen
633 tensions. *BMC Musculoskelet Disord*. 2013;14:353.

- 634 **39.** Grant JA, Wilde J, Miller BS, Bedi A. Comparison of inside-out and all-inside techniques
635 for the repair of isolated meniscal tears: a systematic review. *The American journal of*
636 *sports medicine*. 2012;40:459-468.
- 637 **40.** Longo UG, Campi S, Romeo G, Spiezia F, Maffulli N, Denaro V. Biological strategies to
638 enhance healing of the avascular area of the meniscus. *Stem Cells Int*.
639 2012;2012:528359.
- 640 **41.** Dean CS, Chahla J, Mitchell JJ, LaPrade RF. Outcomes Following Biologically
641 Augmented Isolated Meniscal Repairs with Marrow Venting are Comparable to Meniscal
642 Repairs with Concomitant ACL Reconstruction. *American Journal of Sports Medicine*.
643 2016;In Press
- 644 **42.** Cinque ME, DePhillipo NN, Moatshe G, et al. Clinical Outcomes of Inside-Out Meniscal
645 Repair According to Anatomic Zone of the Meniscal Tear. *Orthop J Sports Med*.
646 2019;7:2325967119860806.
- 647 **43.** Noyes FR, Chen RC, Barber-Westin SD, Potter HG. Greater than 10-year results of red-
648 white longitudinal meniscal repairs in patients 20 years of age or younger. *Am J Sports*
649 *Med*. 2011;39:1008-1017.
- 650 **44.** Huang TL, Lin GT, O'Connor S, Chen DY, Barmada R. Healing potential of experimental
651 meniscal tears in the rabbit. Preliminary results. *Clin Orthop Relat Res*. 1991:299-305.
- 652 **45.** Baldwin J, Wagner F, Martine L, et al. Periosteum tissue engineering in an orthotopic in
653 vivo platform. *Biomaterials*. 2017;121:193-204.
- 654 **46.** Histed SN, Lindenberg ML, Mena E, Turkbey B, Choyke PL, Kurdziel KA. Review of
655 functional/anatomic imaging in oncology. *Nuclear medicine communications*.
656 2012;33:349.
- 657 **47.** Schrepfer S, Deuse T, Reichenspurner H, Fischbein M, Robbins R, Pelletier M. Stem
658 cell transplantation: the lung barrier. *Transplantation proceedings*. Vol 39: Elsevier;
659 2007:573-576.
- 660 **48.** Lu Z, Furumatsu T, Fujii M, Maehara A, Ozaki T. The distribution of vascular endothelial
661 growth factor in human meniscus and a meniscal injury model. *J Orthop Sci*.
662 2017;22:715-721.
- 663 **49.** Crisan M, Yap S, Casteilla L, et al. A perivascular origin for mesenchymal stem cells in
664 multiple human organs. *Cell Stem Cell*. 2008;3:301-313.
- 665 **50.** Anderson AF, Irrgang JJ, Dunn W, et al. Interobserver reliability of the International
666 Society of Arthroscopy, Knee Surgery and Orthopaedic Sports Medicine (ISAKOS)
667 classification of meniscal tears. *The American journal of sports medicine*. 2011;39:926-
668 932.



1) MSC Prevalence

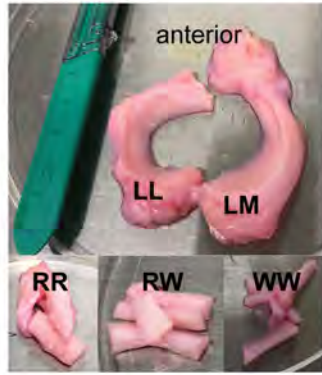


2) Vascularity

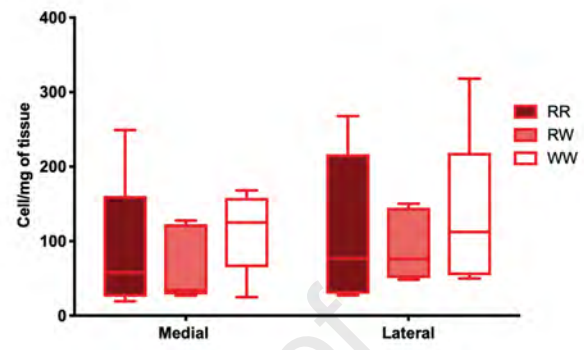


Journal Pre-proof

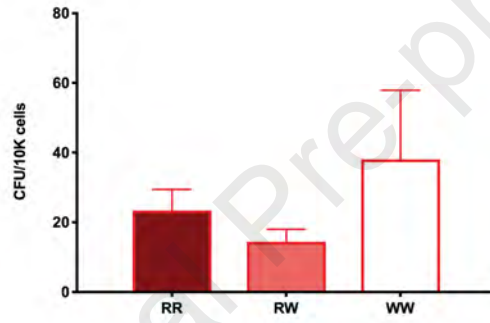
A

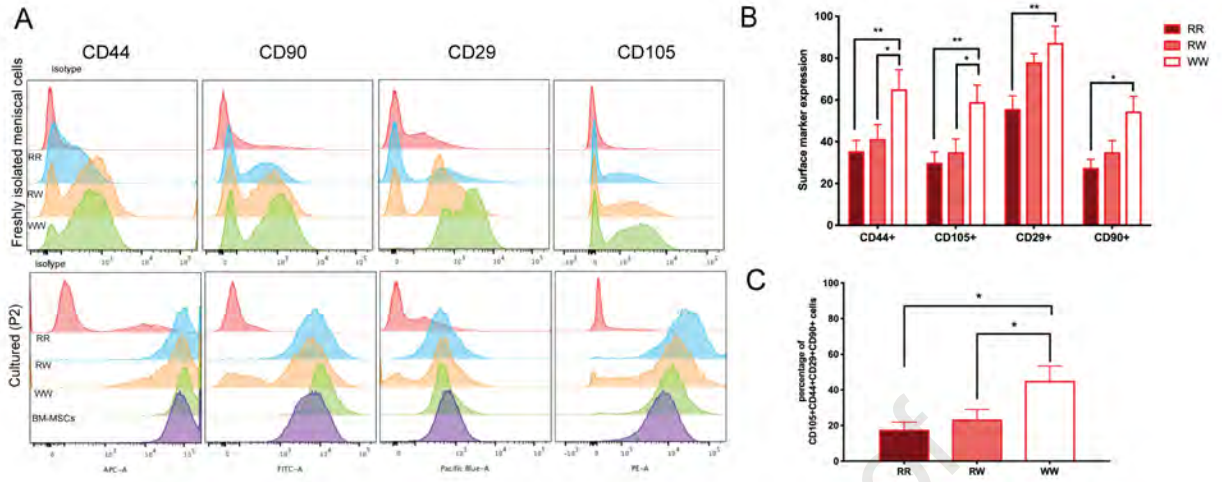


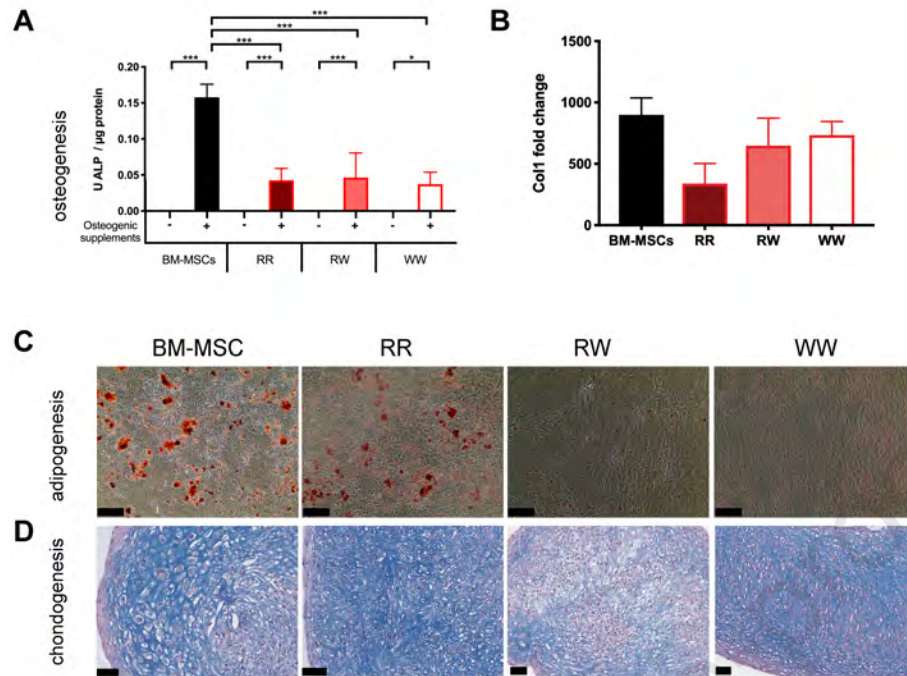
B

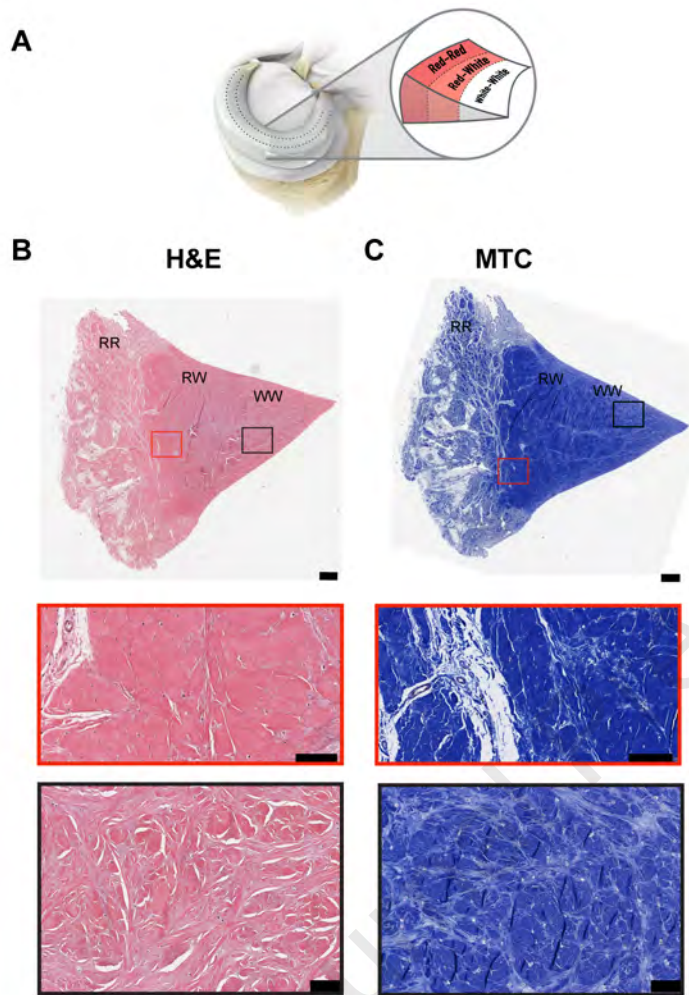


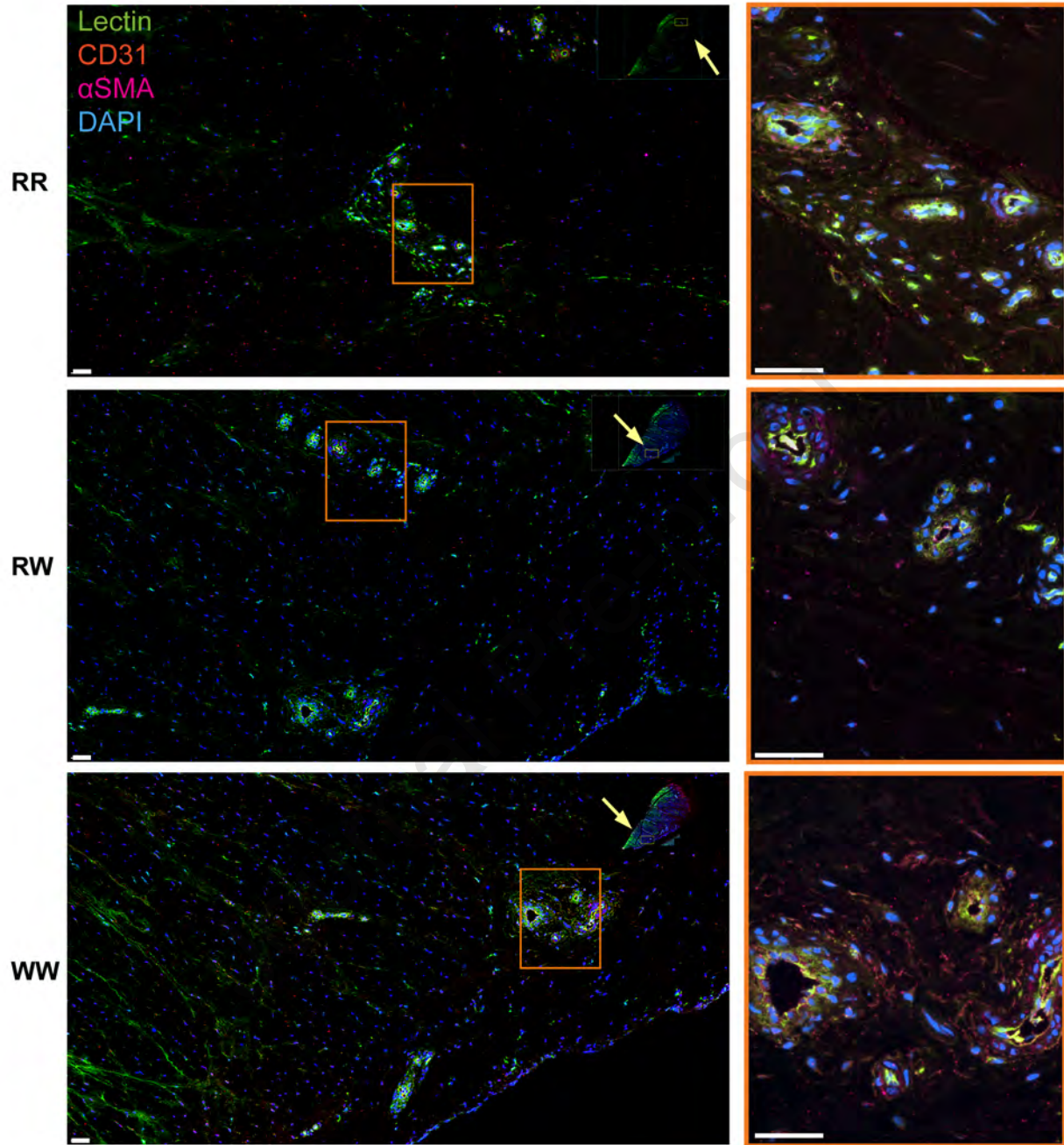
C

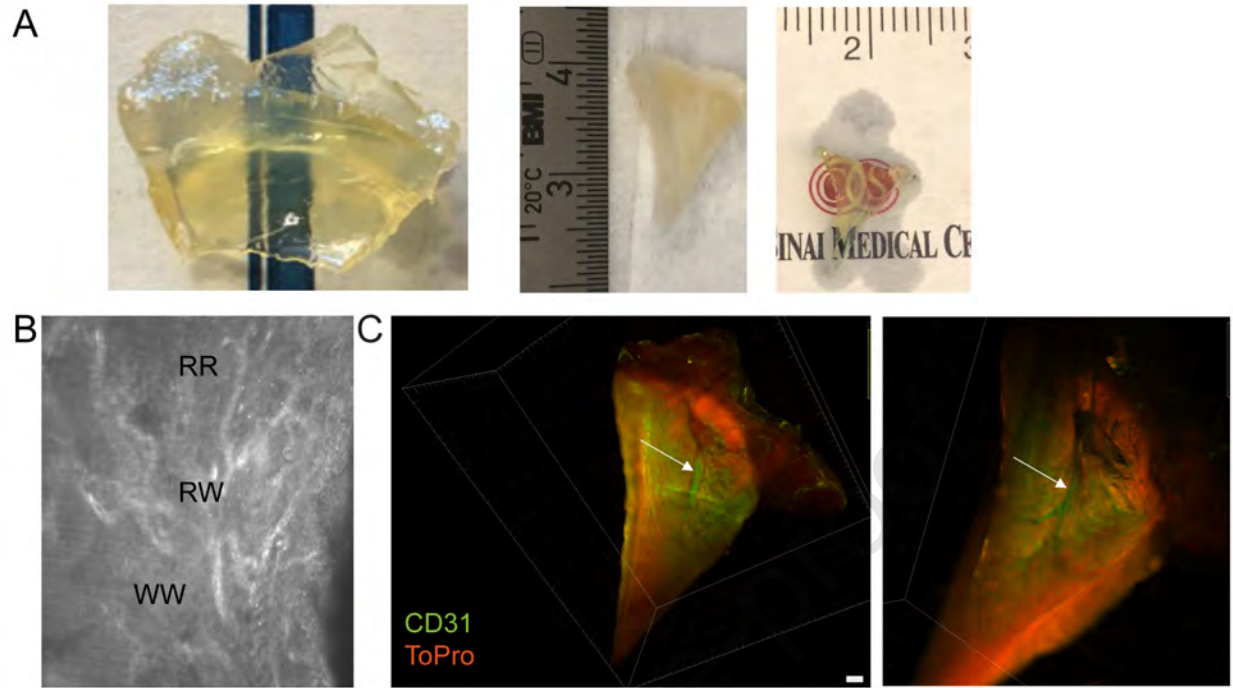












Authorship justification:

1. **Jorge Chahla, MD PhD:** Substantial contributions to the conception and design of the work, drafting the work for important intellectual content, interpretation of data for the work, final approval of the version to be published and agreement to be accountable for all aspects of the work in ensuring that questions related to the accuracy or integrity of any part of the work are appropriately investigated and resolved.
2. **Angela Papalamprou, PhD:** Substantial contributions to the conception and design of the work, acquisition, analysis, or interpretation of data for the work, drafting the work for important intellectual content, final approval of the version to be published and agreement to be accountable for all aspects of the work in ensuring that questions related to the accuracy or integrity of any part of the work are appropriately investigated and resolved.
3. **Virginia Chan, BS:** Substantial contributions to acquisition and analysis for the work, drafting the work for important intellectual content, final approval of the version to be published and agreement to be accountable for all aspects of the work in ensuring that questions related to the accuracy or integrity of any part of the work are appropriately investigated and resolved.
4. **Yasaman Arabi, BS:** Substantial contributions to acquisition and analysis for the work, drafting the work for important intellectual content, final approval of the version to be published and agreement to be accountable for all aspects of the work in ensuring that questions related to the accuracy or integrity of any part of the work are appropriately investigated and resolved.
5. **Khosrawdad Salehi, BS:** Substantial contributions to acquisition and analysis for the work, drafting the work for important intellectual content, final approval of the version to be published and agreement to be accountable for all aspects of the work in ensuring that questions related to the accuracy or integrity of any part of the work are appropriately investigated and resolved.
6. **Trevor J. Nelson, BS:** Substantial contributions to acquisition and analysis for the work, drafting the work for important intellectual content, final approval of the version to be published and agreement to be accountable for all aspects of the work in ensuring that questions related to the accuracy or integrity of any part of the work are appropriately investigated and resolved.
7. **Orr Limpisvasti, MD:** Substantial contributions to the conception of the work, final approval of the version to be published and agreement to be accountable for all aspects of the work in ensuring that questions related to the accuracy or integrity of any part of the work are appropriately investigated and resolved.
8. **Bert R Mandelbaum, MD DHL:** Substantial contributions to the conception of the work, final approval of the version to be published and agreement to be accountable for all aspects of the work in ensuring that questions related to the accuracy or integrity of any part of the work are appropriately investigated and resolved.
9. **Wafa Tawackoli, PhD:** Substantial contributions to the conception and design of the work, drafting the work or revising it critically for important intellectual content, final approval of the version to be published and agreement to be accountable for all aspects of the work in ensuring that questions related to the accuracy or integrity of any part of the work are appropriately investigated and resolved.
10. **Melodie F. Metzger, PhD:** Substantial contributions to the conception and design of the work, drafting the work or revising it critically for important intellectual content, final approval of the version to be published and agreement to be accountable for all aspects of the work in ensuring that questions related to the accuracy or integrity of any part of the work are appropriately investigated and resolved.
11. **Dmitriy Sheyn, PhD:** Substantial contributions to the conception and design of the work, acquisition, analysis, or interpretation of data for the work, drafting the work or revising it critically for important intellectual content, final approval of the version to be published and agreement to be accountable for all aspects of the work in ensuring that questions related to the accuracy or integrity of any part of the work are appropriately investigated and resolved.